Room temperature, continuous wave operation of distributed feedback quantum cascade lasers with widely spaced operation frequencies

Andreas Wittmann,   Marcella Giovannini, and Jérôme Faist[a]
Institute of Physics, University of Neuchâtel, CH-2000 Neuchâtel, Switzerland

Lubos Hvozdara and Stéphane Blaser
Alpes Lasers SA, 1-3 Maximilien-de-Meuron, CH-2000 Neuchâtel, Switzerland

Daniel Hofstetter
Institute of Physics, University of Neuchâtel, CH-2000 Neuchâtel, Switzerland

Emilio Gini
FIRST Center for Micro- and Nanoscience, Swiss Federal Institute of Technology, CH-8093 Zurich, Switzerland

Lasing properties of room temperature, continuous wave operated distributed feedback (DFB) quantum cascade lasers are reported. A bound-to-continuum active region was used to generate a broad gain spectrum. As a result, first-order DFB lasers employing different periods allowed us to achieve single mode continuous wave emission at several wavelengths ranging from 7.7 to 8.3 μm at a temperature of +30 °C. The frequency span corresponds to 8% of the center frequency.

Quantum cascade (QC) distributed feedback (DFB) lasers[1,2] operating in continuous wave (cw) with narrow linewidths (<3.5 MHz) are very promising light sources for many chemical sensing applications, ranging from industrial process control to environmental science and medical diagnostics.[3] DFB-QC lasers operating in cw were reported to emit at 4.8 μm up to 60 °C while lasers at 9.6 μm operated up to 50 °C.[4,5] The relatively small temperature tuning range of a single device usually limits the possibilities of gas analysis. This is particularly true for complex mixtures with multiple absorption lines or in mixtures with very broad lines (typically those with a liquid phase matrix). A device integrating several lasers emitting at different wavelengths would thus allow for the construction of a multichannel laser spectrometer suitable for tracing the analytes in those cases. Ideally, such a device would contain a QC structure with a broad gain spectrum and, if possible, use several emission wavelengths in a monolithic integration concept. Owing to the presence of a miniband-type lower lasing level, the bound-to-continuum active region[6] exhibits a gain spectrum with a full width at half maximum (FWHM) in the range of 200–300 cm^{-1}.[7] This miniband allows for multiple optical transitions with reasonably high oscillator strengths. In this letter, we therefore investigate the lasing characteristics of a series of monolithically integrated DFB lasers using a bound-to-continuum active region and differing in the grating period only.

The fabrication procedure of these lasers started with molecular beam epitaxy of a 220 nm thick InGaAs lower confinement layer, an InGaAs/InAlAs based active region, and a 310 nm thick InGaAs upper confinement layer. All these layers were lattice matched to the InP substrate. The bound-to-continuum active region consisted of 35 periods and was optimized for an emission maximum at 1270 cm^{-1}. The relevant wave functions and one period of the conduc-

tion band structure are plotted in Fig. 1. The thicknesses and doping levels are described in the figure caption. The substrate is a n-doped, (100)-oriented InP wafer [S, $(1-2) \times 10^{17}$ cm^{-3}] whereas the two confinement layers are low n-doped InGaAs (Si, 4×10^{16} cm^{-3}). The DFB gratings with periods ranging from 1.185 to 1.305 μm were defined using a single photolithography step and wet etched into the top confinement layer. In order to have access to a large portion of the gain spectrum, 25 different grating periods were fabricated on one chip. Subsequently, the 170 nm deep gratings were overgrown by metal organic vapor phase epitaxy with a 4 μm thick InP cladding layer (Si, 1×10^{17} cm^{-3}) and two 15 nm thick quaternary InGaAsP layers (Si, 1×10^{18} cm^{-3}), whose band gaps corresponded to photoluminescence maxima of 1.1 and 1.28 μm, respectively. Their purpose was to reduce the total series resistance of the device. Finally, the
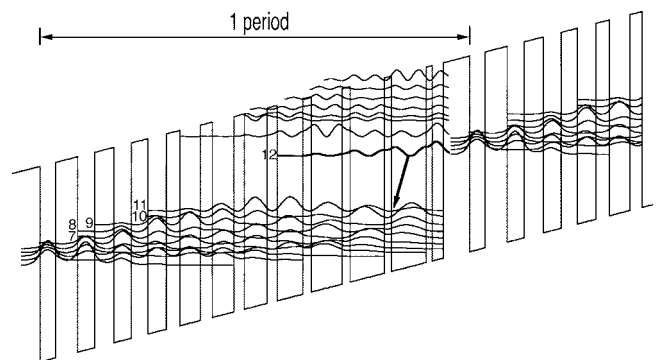

FIG. 1. Quantum well structure of the bound-to-continuum design under an applied electric field of 4.5×10^4 V/cm. The moduli squared of the relevant wave functions (in bold the upper state of lasing transition) are plotted and the arrow indicates the radiative transition. The layer sequence of one active cell, given in nanometers and starting from the injector barrier, is **4.2**/1.7/**0.9**/5.3/**1.1**/5.2/**1.2**/4.7/**1.3**/3.9/**1.5**/3.5/**1.6**/3.3/**1.8**/3.1/**2.1**/2.8/**2.5**/2.7/**2.9**/2.6/**3.3**/2.4, where InAlAs barriers are in bold, InGaAs are in roman, and underlined numbers correspond to the n-doped layers (Si, 8×10^{16} cm^{-3}).
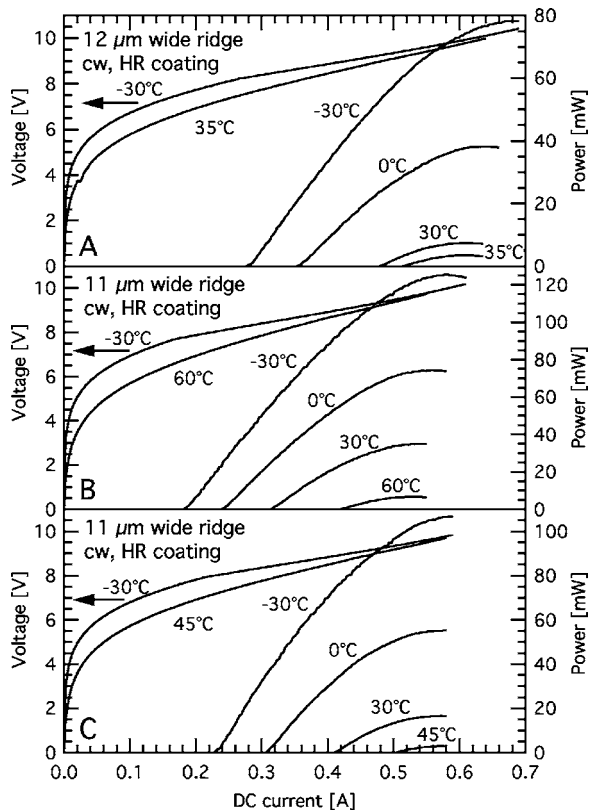
[a]Electronic mail: wittmann@phys.ethz.ch

FIG. 2. Optical power and voltage vs dc current of samples A, B, and C at different heatsink temperatures. Sample B is close to the center of the gain curve, and samples A and C are located towards the lower/upper limits of available frequency range (corresponding spectra in Fig. 3).
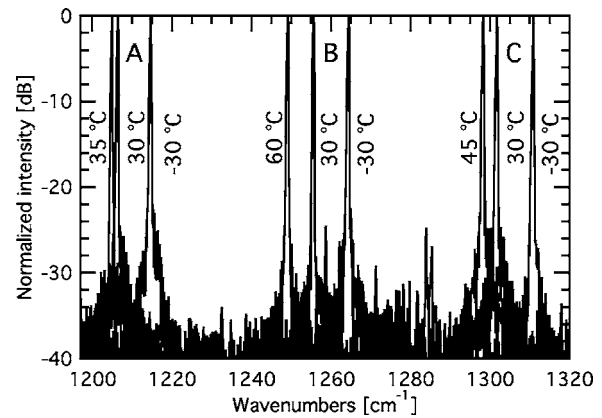

FIG. 3. High resolution single mode cw spectra of samples A, B, and C showing operation with a side-mode suppression ratio >25 dB. Depicted are the spectra at 1.1× threshold and 30 °C and at the extremes of single laser tuning range achieved by the variation of temperature tuning. The corresponding single tuning ranges for samples A, B, and C are 10, 15, and 12 cm^{-1}, respectively.

growth was terminated by a 300 nm thick plasmon layer[8] (Si, 9×10^{18} cm^{-3}) and a 50 nm thick, highly doped contact layer (Si, 2×10^{19} cm^{-3}), both consisting of lattice matched InGaAs. Subsequently, DFB lasers were fabricated by standard lithography processes and wet etching. After evaporation of the contacts, a 3 μm thick layer of gold was electroplated on the top in order to improve the heat dissipation of the device. After cleaving into 1.5 mm long laser bars, a high reflection coating with a reflectivity of $R \approx 97\%$ was evaporated on the back facet. All lasers were mounted junction up onto copper heatsinks using In solder.

For characterization in terms of light output, the laser power was measured using a calibrated thermopile detector. Spectra were recorded using a Fourier transform infrared spectrometer (Bruker Vertex 70) equipped with a deuterated triglycine sulphate detector. The laser was mounted on a thermoelectric cooler. For the discussion of the optical and spectral characterizations, we chose three samples with three different grating periods (A: 1.3 μm, B: 1.25 μm, and C: 1.2 μm, out of the 25 fabricated). The Bragg resonance of sample B lies close to the center of the gain curve whereas samples A and C are located towards the upper/lower limits of the available wavelength range.

Figure 2 shows a series of *L-I-V*-curves for all three lasers. At a temperature of +30 °C, we observe a maximum output power and a slope efficiency of 35 mW and 245 mW/A for laser B, whereas A and C show lower powers and slope efficiencies. In addition, sample B reaches a maximum operation temperature of 60 °C while samples A and C stop lasing cw at 35 and 45 °C, respectively.

In Fig. 3, we show cw emission spectra of the three

devices at different heatsink temperatures. At +30 °C, we observed emission energies (wavelengths) of 1206 cm^{-1} (8.3 μm), 1256 cm^{-1} (8.0 μm), and 1302 cm^{-1} (7.7 μm), respectively. Taking into account the temperature tuning range of samples A and C leads to a total wavelength coverage of more than 100 cm^{-1} (i.e., 8% of the center frequency). Stable single mode cw operation with a side-mode suppression ratio >25 dB was observed within the entire examined frequency and temperature range.

Figure 4 is a scatter graph of the threshold current density values of all investigated lasers at +30 °C. Although the plot contains data for different ridge widths as well as intermediate grating periods (not belonging to class A, B, or C), one can clearly see the overall trends. The threshold current densities increase from 1.87 kA/cm^2 (sample B) to 2.62 kA/cm^2 (sample A) and 2.45 kA/cm^2 (sample C).

In Fig. 5, finally, we compare the electroluminescence spectrum with a computed luminescence spectrum and the normalized inverse threshold current densities of the three samples A, B, and C. The electroluminescence was measured under an applied bias voltage of 9.6 V, a duty cycle of 4%, and a temperature of 300 K. It exhibits a large full width at half maximum of 274 cm^{-1}, which corresponds to a relative width of $\Delta v/v_0 = 21\%$. This is in good agreement with the
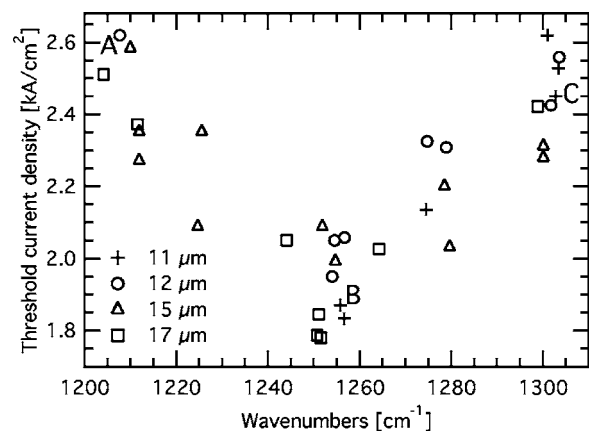

FIG. 4. Threshold current density in cw operation at +30 °C vs wave numbers. The threshold current densities increase from 1.87 kA/cm^2 (sample B) to 2.45 kA/cm^2 (sample C) and 2.62 kA/cm^2 (sample A).
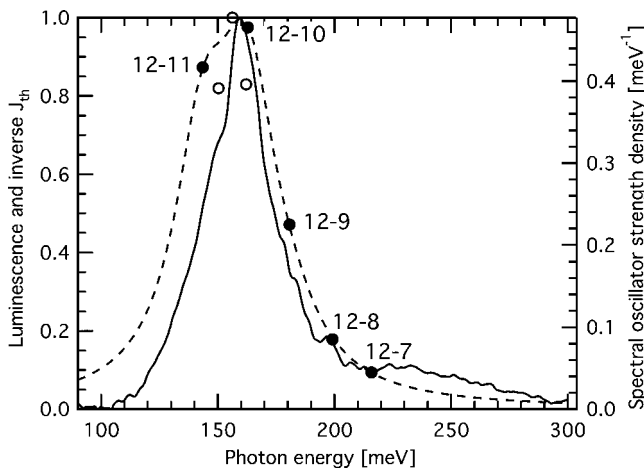
FIG. 5. Solid line: Normalized electroluminescence spectrum at 300 K measured under an applied bias voltage of 9.6 V. Dashed line: Sum of computed oscillator strengths of the transitions from level 12, assuming a Lorentzian broadening of 30 meV FWHM for each transition. Open circles: Normalized inverse threshold current density of the three samples A, B, and C measured in pulsed mode.

line shape obtained by summing the computed oscillator strengths of the various transitions (12-11, 12-10, 12-9, 12-8, and 12-7), which are labeled in Fig. 1, and assuming Lorentzian broadening with a FWHM of 30 meV.[9] The transition 12-11 is most likely overestimated due to dephasing scattering (see Ref. 9).

In order to get a fair comparison between the threshold values and the electroluminescence, samples A, B, and C were measured in pulsed mode as well. Their inverse threshold current densities at 2% duty cycle, normalized to sample B, are also plotted in Fig. 5. We thereof observe a slight red-shift of the gain with respect to the luminescence spectrum. Since the applied biases were similar, we tentatively attribute this shift to second-order gain mechanisms.[10,11] Nevertheless, the overall behavior leads to the conclusion that the gain must have its maximum close to the Bragg resonance of sample B.

An interesting question is obviously how far away from the gain center such a DFB laser could still yield single mode operation. For single mode operation, the mode discrimination $\Delta\alpha$ must be larger than the threshold gain difference Δg. For sufficiently separated modes, $\Delta\alpha$ is the difference between the threshold gain g_{th} of the Fabry-Pérot (α_{FB} =4.47 cm^{-1}) and of the DFB cavity (α_{DFB}=0.7 cm^{-1}), estimated to $\Delta\alpha$=3.8 cm^{-1}. The threshold gain, which can be expressed by $g_{th}(v,J)=Jg_D(v)$, must compensate the total losses of the laser. For two DFB lasers with different emission wavelengths but using the same gain material, we then find $g_D(v_A)/g_D(v_B)=J_{th,B}/J_{th,A}$. From the measured value of this ratio $g_D(v_A)/g_D(v_B)=0.82$ from samples A and B and the computed waveguide losses $\alpha_w=3.4$ cm^{-1}, we extrapolate a threshold gain difference $\Delta g=0.7$ cm^{-1}. As a consequence, single mode operation could be in principle achieved over an even wider frequency range.

Thermal resistances R_{th} and thermal tuning coefficients $\beta=(1/v)(\Delta v/\Delta T)$ for samples A, B, and C were extracted from the spectral characteristics.[12] We compute an average thermal tuning coefficient $\beta=-8.88\times10^{-5}$ K^{-1} and an average thermal resistance R_{th} of 12.4 K/W, which corresponds to an average specific conductance of 455 W/(K cm^2). The thermal resistance of sample B was also calculated from the comparison of threshold currents in cw and pulsed operations. A thermal resistance of 18.1 K/W was found. The higher value obtained with this method compared to the spectral analysis is due to the nonunity "thermal overlap" factor of the active region and is comparable with literature values.[4,12] Fitting finally the threshold current versus temperature curve by the empirical formula $I_{th}=I_0\exp(T/T_0)$ leads to $T_0=157$ K and $I_0=0.0339$ A for pulsed operation and $T_0=107$ K and $I_0=0.0185$ A for cw operation. From the pulsed values, one can estimate the maximally reachable cw temperature $T_{max}=T_0[\ln(T_0(R_{th}V_{op}I_0)^{-1})-1]$.[13] By taking R_{th} =18.1 K/W and $V_{op}=10$ V, one ends up with $T_{max}=352$ K (79 °C), which is in reasonable agreement with the measured maximum cw temperature of 333 K (60 °C).

In conclusion, we demonstrated room temperature cw operation of QC lasers based on the bound-to-continuum design. By exploiting its broad gain peak and DFB gratings with 25 different periods, we were able to achieve single mode emission at wavelengths ranging from 7.7 to 8.3 μm from a single processing run, i.e., from one piece of material. The results show the usability of the bound-to-continuum design for the integration of monolithically integrated high-performance DFB lasers emitting at different wavelengths. Such devices have applications in multichannel laser spectrometers.

[1]J. Faist, C. Gmachl, F. Capasso, C. Sirtori, D. L. Sivco, J. N. Baillargeon, and A. Y. Cho, Appl. Phys. Lett. **70**, 2670 (1997).
[2]C. Gmachl, A. Straub, R. Colombelli, F. Capasso, D. Sivco, A. Sergent, and A. Cho, IEEE J. Quantum Electron. **38**, 569 (2002).
[3]A. Kosterev and F. Tittel, IEEE J. Quantum Electron. **38**, 582 (2002).
[4]J. Yu, S. Slivken, S. Darvish, A. Evans, B. Gokden, and M. Razeghi, Appl. Phys. Lett. **87**, 041104 (2005).
[5]S. R. Darvish, S. Slivken, A. Evans, J. S. Yu, and M. Razeghi, Appl. Phys. Lett. **88**, 201114 (2006).
[6]J. Faist, M. Beck, T. Aellen, and E. Gini, Appl. Phys. Lett. **78**, 147 (2001).
[7]R. Maulini, D. A. Yarekha, J.-M. Bulliard, M. Giovannini, J. Faist, and E. Gini, Opt. Lett. **30**, 2584 (2005).
[8]C. Sirtori, J. Faist, F. Capasso, D. L. Sivco, A. L. Hutchinson, and A. Y. Cho, Appl. Phys. Lett. **66**, 3242 (1995).
[9]R. Maulini, M. Beck, J. Faist, and E. Gini, Appl. Phys. Lett. **84**, 1659 (2004).
[10]H. Willenberg, G. H. Döhler, and J. Faist, Phys. Rev. B **67**, 085315 (2003).
[11]R. Terazzi, T. Gresch, M. Giovannini, N. Hoyler, J. Faist, and N. Sekine (unpublished).
[12]S. Blaser, D. Yarekha, L. Hvozdara, Y. Bonetti, A. Muller, M. Giovannini, and J. Faist, Appl. Phys. Lett. **86**, 41109 (2005).
[13]M. Beck, D. Hofstetter, T. Aellen, J. Faist, U. Oesterle, M. Ilegems, E. Gini, and H. Melchior, Science **295**, 301 (2002).